Techno-Economic Potential and Perspectives of Floating Photovoltaics in Europe

Leonardo Micheli [1,2], Diego L. Talavera [3], Giuseppe Marco Tina [4], Florencia Almonacid [2], Eduardo F. Fernández [2]*

[1] Dept. of Astronautical, Electrical and Energy Engineering (DIAEE), Sapienza University of Rome, Rome, Italy
[2] Advances in Photovoltaic Technology (AdPVTech), CEACTEMA, University of Jaén, Jaén, Spain
[3] IDEA Research Group, University of Jaén, Jaén, Spain
[4] Department of Electrical, Electronic and Computer Engineering, University of Catania, Catania, Italy
*** Corresponding author**: L. Micheli, Leonardo.micheli@uniroma1.it

Highlights

- The energy and economic potential of floating photovoltaics in Europe is estimated.
- Photovoltaic modules on 1% of the water surface would raise the EU capacity by 11%.
- Floating Photovoltaics (FPV) is best performing in southern EU countries.
- The cost-competitiveness of FPV strongly depends on its thermal behavior.
- FPV could be favored by limiting "Racking & mounting" and "Grid Connection" costs.

Abstract

In floating photovoltaics, modules are installed on water in order to limit the land occupancy, an issue arising with the growing deployment of photovoltaics. The floating structures are also expected to lower the capital expenditures required by traditional in-land systems, thanks to the easier installation and to the hybridization with hydropower plants. This work estimates the yield potential and the cost effectiveness of floating photovoltaics across suitable water bodies in Europe compared to optimally tilted land-based photovoltaics. Energy and economic outputs are modelled using referenced models, field-measured parameters and considering weather and economic conditions specific to each location and each country. The results show that, despite the lower tilts and thanks to the better thermal performance, floating photovoltaics can achieve energy yields up to 2% greater than land-based photovoltaics. This is especially true in the Mediterranean region, where the average position of the Sun and the temperatures are higher. In addition, it is found that, even when underperforming, floating photovoltaics can be cost competitive with land-based photovoltaics if the installation costs are reduced by less than 12%. Last, this study estimates that each additional degree of tilt angle in floating photovoltaics installations is worth between 2.5 and 7.5 €/kW.

Graphical abstract

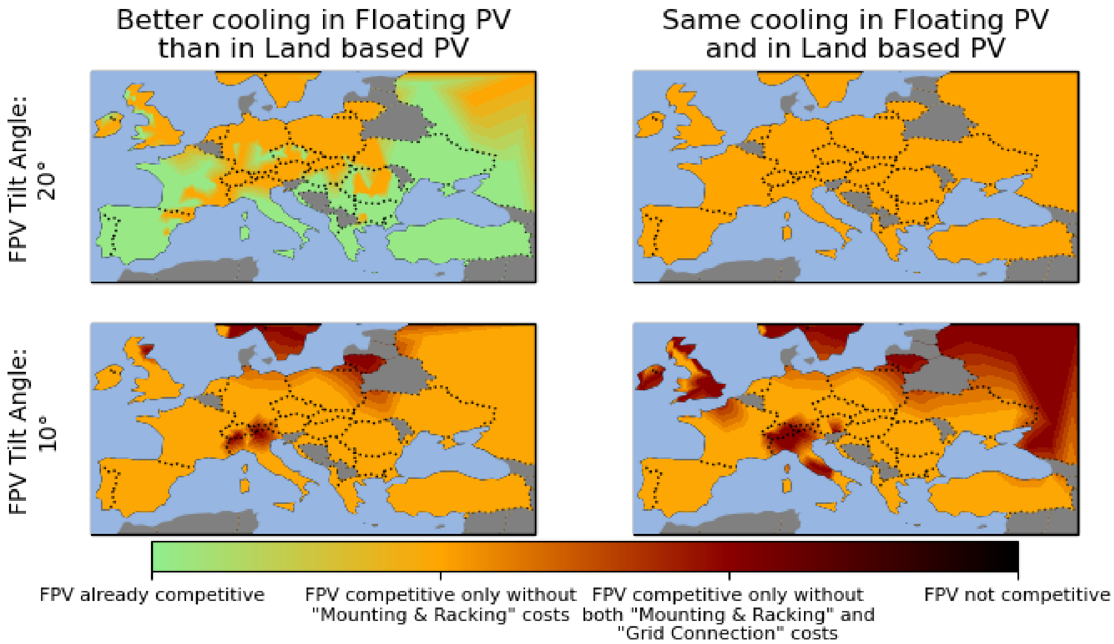

Keywords

Floating photovoltaics; Energy yield; Energy cost; LCOE; Europe; Techno-economic analysis

1. Introduction

Increasing the share of affordable and clean energy is among the United Nations Sustainable Development Goals for 2030 (Department of Economic and Social Affairs, 2016). Pushed by low-cost, easiness of installation and versatility, photovoltaics (PV) is one of the renewable energies growing faster and expected to majorly contribute to this renewable energy shift (SolarPower Europe, 2020).

In order to reduce their carbon footprints and their dependance on fossil sources, the European member states plan building between 140 and 222 GW of new PV power plants by 2030 (Kougias et al., 2021). This means that 14 to 22 GW of new PV capacity will be installed every year until 2030. At an approximate rate of 0.02 km^2 per MW (Álvarez and Zafra, 2021), this will require the conversion of 280 to 440 km^2 (28000 to 44000 ha) of land into PV facilities every year. This major land conversion is concerning because it can threaten biodiversity, as PV plants might be installed on land available for low prices but of high ecological value (Serrano et al., 2020). This issue is particularly significant in Europe, the continent that has already the highest number of renewable systems installed in protected areas (Rehbein et al., 2020). Aware of the potential risks for the environment, the European commission now specifically requires research and innovation activities not to make any significant harm to biodiversity and ecosystems (Marino, 2021). In addition to these threats to biodiversity, the significant investments in PV and the high expected profits could also lead to the conversion of arable land into solar parks, potentially generating conflicts with agriculture as well (Späth, 2018). Therefore, innovative solutions are needed to avoid that EU and/or global energy goals are met at the expenses of biodiversity and/or food production.

One of the solutions to this land occupancy issue is floating photovoltaics (FPV), in which PV modules are installed on water surfaces rather than on land. In addition to avoiding land-use competition, FPV has the potential to achieve lower costs than traditional land-based PV (LPV), because of the easier installation and the lower rent fees of water compared to land (World Bank Group et al., 2018). The cost reduction is expected to be even greater when FPV is coupled with hydropower because, in this hybrid configuration, FPV can make use of existing electrical infrastructures (World Bank Group et al., 2018). Moreover, FPV can reduce the evaporation rates, making more water available for other uses, such as irrigation or hydropower generation (Bontempo Scavo et al., 2021). Last, thanks to the cooling effect of water, FPV modules have been often reported to work at lower temperatures than LPV (Kumar et al., 2021). This means that, because of the inverse relationship between temperature and efficiency, FPV can achieve higher yields than LPV. However, researchers have recently started pointing out that these temperature benefits are not universal as they depend on the system's configuration and on the local conditions. For example, a study conducted in Cambodia (Peters and Nobre, 2022) found the FPV system working at higher temperatures than a nearby LPV system. The result was attributed to the lower wind speeds registered on that basin compared to land. An analysis of FPV systems deployed in the Netherlands and in Singapore showed that some FPV geometries do not achieve better thermal behaviors than LPV (Dörenkämper et al., 2021). Therefore, modelers and analysists cannot assume that FPV would always work at lower operating temperatures than LPV. In addition, they should take into account that, due to the lack of foundation, FPV modules are typically installed at low tilt angles to limit the wind load on the supporting structure (Silvério et al., 2018). At European latitudes, this low inclination increases the reflection and angular losses compared to the optimal angle, reducing the effective irradiance reaching the PV cell and therefore the energy yield.

Because of the potential advantages, the expected profits and the lack of land-use competition, a significant capacity of FPV has been deployed in the recent years (Rosa-Clot and Tina, 2020), reaching 2.6 GW installed worldwide until mid-2020 (Haugwitz, 2020). The global potential for FPV systems deployed in hydropower basins is estimated in between 3.0 and 7.6 TW (Lee et al., 2020). This means that FPV can play a key role in the renewable energy shift of several countries. Indeed, it has been estimated that it could provide up to 10% of the national electricity consumption of the U.S., if 27% of the surface of suitable man-made water basins in the country was covered with modules (Spencer et al., 2019). A different study calculated that, with less than 1% of the surface of the largest African reservoirs covered by modules, FPV could increase the hydropower electricity output of the continent by 58% (Gonzalez Sanchez et al., 2021). Even if Asia has so far represented the major market for FPV (Haugwitz, 2020), this technology can be expected to contribute also to the achievements of the European energy goals. For example, it was recently shown that Spain could achieve 70% of its 2030 PV targets just by integrating FPV on the available hydropower basins (Micheli, 2021). Nonetheless, despite this potential, an investigation on the possible FPV capacity and yield in Europe has not been presented yet.

Despite the aforementioned advantages, the success of FPV will not be solely dependent on the available water surface and on the energy yield. Indeed, it will strongly depend also on its costs, especially compared to those of LPV. Given the young age of the technology, the costs of FPV are still high, due to the early stage of its economy of scale and supply chain (World Bank Group et al., 2018). However, a life cycle assessment analysis estimated lower costs of electricity and similar payback periods for FPV compared to polycrystalline LPV in Thailand (Cromratie Clemons et al., 2021). Similar payback periods for FPV and LPV were reported for a semiarid region of Brazil (Padilha Campos Lopes et al., 2020). While still of significance, these previous works considered fixed performance ratios and/or fixed improved efficiencies for FPV over LPV under the assumption of a water-cooling effect. As discussed, in reality, the thermal behavior of FPV will change with the system's design and it cannot be always considered better than that of LPV. Furthermore, the performance will change depending on the irradiance and weather conditions of each site. Last, one should take into account the additional losses due to the lower tilt angles at which FPV are typically mounted compared to LPV.

It should be also noted that the cost competitiveness of FPV would vary depending on the economic conditions of each specific country. Indeed, FPV can lower the costs of selected categories of the PV Balance of System, such as Racking and Mounting, due to the lack of major foundation works, or Grid connection, if existing hydroelectric infrastructures are used. The weight of these categories on the PV capital costs varies from country to country (IRENA, 2021). Therefore, it is essential understanding how the different balance of system cost breakdowns can affect the competitiveness of FPV in different countries.

In light of the ambitious plans to install tens of new GW of PV in the current decade and of the need of alternative solutions to preserve biodiversity and arable land, the present work aims to assess the expected energy and economic performance of floating PV in Europe against that of traditional LPV. Previous assessments conducted at global-scale or in different regions have made use of land-based PV capacity factors to estimate the production of FPV modules or have assumed the same performance ratios for all locations. Differently from these works, the present analysis calculates the energy yields of FPV and LPV systems in the various European countries using field-measured parameters specific to each technology and hourly satellite-derived weather data for each individual location. This way, realistic comparisons can be made, and the generated yields can be used to identify the environmental factors that can favor the FPV deployment.

The economic analysis is conducted by calculating the maximum capital expenditure (CAPEX) that FPV could face to be cost competitive with traditional photovoltaic systems. In other words, the scope of the work is the estimation of the maximum FPV capital expenditure ($CAPEX_{FPV}$) so that:

$$LCOE_{FPV}(CAPEX_{FPV}) \leq LCOE_{LPV}(CAPEX_{LPV}) \quad (1)$$

where LCOE is the Levelized Cost of Electricity, an index that measures the cost of each kWh of electricity produced by a system over its lifetime. A similar aim was pursued in (Micheli, 2021), which was, however, limited to Spain and to a single FPV configuration. The present analysis is not a mere geographical extension of that previous work. Indeed, as aforementioned, multiple scenarios and a more detailed economic analysis are presented here, taking into account the actual PV capital expenditure breakdown in the various countries. This way, the performance of FPV can be discussed in light of each country's specific conditions and costs.

Overall, this work presents a first estimation of the costs and benefits of FPV for different thermal behaviors and tilt configurations in light of the most recent findings, realistic data, and the specific economics of various European countries. The large number of analyzed data points makes it possible to identify environmental and economic conditions that can favor the deployment of this technology. The results show the cost reductions that should be targeted to make FPV cost-competitive with land-based photovoltaics and the additional expenses that can be sustained to increase the yield of FPV systems. In addition, the proposed methodology can be easily re-applied in future, as new data become available in the literature, or also immediately used for different regions.

2. Methods

The methodology employed in this work is detailed in the following subsections and described in the flowchart in Fig. 1.

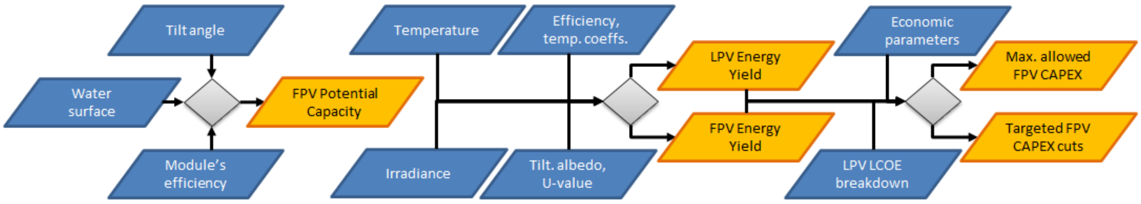

Fig. 1. Schematic of the methodology and the results of this work.

2.1. FPV Capacity

The FPV capacity was estimated using the water surface data available in the Global Reservoir and Dam Database (GRanD) v1.3 (Lehner et al., 2011) and assuming a spacing between rows 20% larger than the height of the modules from the ground (Micheli, 2021):

$$C_{FPV}(\theta) = \mathrm{A_{res}} \cdot r_{FPV} \cdot \frac{1}{\cos\theta + 1.2 \cdot sin\theta} \cdot \eta \cdot G_{STC} \qquad (2)$$

where $\mathrm{A_{res}}$ is the available reservoir surface, and r_{FPV} is the percentage covered by modules, θ is the tilt angle, η is the electrical efficiency and G_{STC} is the standard the condition irradiance (1000 W/m^2).

The same filters used by (Spencer et al., 2019) were applied to remove duplicate reservoirs (same water surface and same administrative unit), to reflect current industry trends (1ha surface and 2m depth minimum) and to remove reservoirs with potentially conflicting main purposes (i.e. "Recreation", "Navigation", "Fisheries" or "Other"). This way, only the reservoirs mainly used for "Hydroelectricity", "Water supply", "Irrigation" and "Flood control" were considered. The last two filters removed 14% of the reservoirs (19% of the surface), while only 2% of the reservoirs were flagged as potential duplicates (<1% of the surface). In addition, 23% of the remaining sites in the database did not have available all the information required by the filters (i.e., water surface, depth, administrative unit, or main use). In order to maintain a conservative approach, also these sites were removed.

2.2. PV Performance Modelling

The energy yields of a monofacial module were simulated using the PVWatts DC power model (Dobos, 2014) available in pvlib python (Holmgren et al., 2018). The components of the hourly irradiance were downloaded from CAMS Radiation Service (Gschwind et al., 2019; Lefèvre et al., 2013; Qu et al., 2017). These were converted into a plane-of-array irradiance using the Perez model for diffuse irradiance (Perez et al., 1990, 1988, 1987), and a referenced function for the ground-reflected irradiance (Loutzenhiser et al., 2007). The effective irradiance was calculated by correcting the plane-of-array irradiance using the incidence angle modifier described in (De Soto et al., 2006). Relative and absolute air mass values were calculated from the solar position, as in (Gueymard, 1993; Kasten and Young, 1989). The simulation was conducted using the parameters described in Table 1. An albedo of 0.25 was used for the LPV applications, which is the default value in pvlib python (Holmgren et al., 2018), and of 0.06 for

FPV, as experimentally reported by (Liu et al., 2018). Fixed 14% losses were considered to convert DC power into AC, in addition to the loss due to a 96% efficient inverter (Dobos, 2014).

Most of the FPV capacity nowadays belongs to plants > 15 MW (World Bank Group et al., 2019) and is therefore intended for utility-scale purposes. The vast majority of FPV systems are installed at fixed tilt angles (World Bank Group et al., 2018). Because of this, the FPV performances were here compared with those of optimally tilted LPV systems. Only fixed tilt angles were assumed not to compare tracking and non-tracking configurations, which require different costs. The optimal LPV tilt in each location was detected modelling the PV performance for any tilt angle in between 15° and 60° (at 1°-step) and by selecting the angle returning the maximum yield. All modules are modelled as southward oriented.

In order to represent better the variety of designs currently available and because of the weight of the reflection losses on the results, this work takes into account two tilt angle configurations for FPV. According to a recent report (World Bank Group et al., 2019), most of the FPV plants are installed at tilt angles below 15°. For this reason, the first scenario assumes a tilt angle of 10°, the maximum recommended by a previous study for latitudes of Italy, Spain and above (Silvério et al., 2018). This is in line with the 11° angle, “commonly used for FPV installations” according to NREL (Spencer et al., 2019). The second scenario assumes a tilt angle of 20°, one of the highest reported for commercial floaters (World Bank Group et al., 2019).

Table 1. Energy modelling parameters.

	FPV	**LPV**
Tilt angle	10° (Silvério et al., 2018) 20° (World Bank Group et al., 2019)	Optimum
PV Module Efficiency	21.4% (Trina, 2021)	21.4% (Trina, 2021)
PV module temperature coefficient	-0.0034 C^{-1} (Trina, 2021)	-0.0034 C^{-1} (Trina, 2021)
Albedo	0.06 (Liu et al., 2018)	0.25 (Holmgren et al., 2018)
DC to AC Losses	14% (Marion et al., 2005)	14% (Marion et al., 2005)
Inverter efficiency	96% (Marion et al., 2005)	96% (Marion et al., 2005)

The temperature of the PV cell was calculated using the PVsyst’s heat loss factor model (PVsyst SA, n.d.):

$$T_c = T_a + \frac{POA \cdot \alpha \cdot (1 - \eta_{PV})}{U} \qquad (3)$$

where T_a is the ambient temperature, downloaded from ERA-5 (Hersbach et al., 2018), POA is the plane-of-array irradiance and α is the absorption coefficient of solar irradiation (default value: 0.9). The module’s efficiency, η_{PV}, in equation (3) was set to 0.1, as recommended by PVSyst when it cannot be estimated in operating conditions. Last, U is the heat loss coefficient. The higher its value, the better the thermal exchange of the PV module with the environment, and, therefore, the lower its operating temperature. In its original formulation (Faiman, 2008), the U-value is split into a constant and a convective components, and this last one is multiplied by the wind speed. However, PVSyst recommends using the heat loss coefficient U without wind dependency. In addition, limited differences have been reported between the two approaches when used to simulate the field performance of FPV systems (Dörenkämper et al., 2021).

Different studies have reported lower operating temperatures in FPV compared to LPV. A study conducted on a 1MW testbed in Singapore (Liu et al., 2018) reported lower temperatures for all the FPV systems compared to a reference co-located LPV, thanks also to the consistently higher wind speed registered offshore compared to onshore. The authors however highlighted that the FPV module design could favor or obstruct the heat transfer, affecting the U-value of the system. These conclusions were confirmed by a different work (Dörenkämper et al., 2021), which analyzed data from FPV and LPV systems in the Netherlands and Singapore. In this case, U-value as high as 57 W/m^{2}K were found for some specific designs (Dörenkämper et al., 2021). This is almost twice the U-value typically employed for modelling land-based PV. On the other hand, the same work also showed that different FPV configurations could experience the same U-value of LPV. Some authors had previously warned that FPV systems could not necessarily operate at lower temperatures than co-located LPV (Peters and Nobre, 2020). The same concern was shared by the authors of (Lindholm et al., 2021), which developed a thermal model to evaluate the performance for various FPV designs. They found that, if FPV modules are not mounted horizontally and in contact with water, they might not experience any thermal benefit compared to LPV. In order to reflect this ongoing debate on the thermal exchange capacities of FPV, four thermal scenarios were considered in this work, as described in Table 2. These scenarios represent a variety of conditions: from a significantly better thermal exchange for FPV (Scenario A), to FPV only slightly overperforming LPV in terms of heat transfer (Scenarios B and C), to same thermal exchange conditions for FPV and LPV (Scenario D).

Each scenario is obtained as a combination of a FPV U-value and a LPV U-value. For FPV, the heat loss coefficients were set to 56 W/m^{2}K and 39 W/m^{2}K. The first one represents the average of the values reported by (Dörenkämper et al., 2021) for open structures in the Netherlands and Singapore. The second value is in line with those reported by (Dörenkämper et al., 2021; Liu et al., 2018) and it was chosen so that it matched the U-values found by (Dörenkämper et al., 2021; Peters and Nobre, 2020) for land-based systems located nearby water basins. Last, the LPV U-value of 29 W/m^{2}K was selected being the one recommended in PVSyst for well ventilated PV systems (PVsyst SA, n.d.).

Table 2. Combinations of FPV and LPV U-values in the four thermal scenarios considered in this study.

<table>
<tr><td colspan="2" rowspan="2"></td><td colspan="2">FPV U-value</td></tr>
<tr><td>56 W/m^{2}K (Dörenkämper et al., 2021)</td><td>39 W/m^{2}K (Dörenkämper et al., 2021; Liu et al., 2018)</td></tr>
<tr><td rowspan="2">LPV U-value</td><td>29 W/m^{2}K (PVsyst SA, n.d.)</td><td>Scenario A: significantly better cooling in FPV</td><td>Scenario C: better cooling in FPV</td></tr>
<tr><td>39 W/m^{2}K (Dörenkämper et al., 2021; Peters and Nobre, 2020)</td><td>Scenario B: better cooling in FPV</td><td>Scenario D: same cooling in FPV and LPV</td></tr>
</table>

The model makes use of satellite-derived irradiation data to estimate the energy yield and the LCOE of the LPV and FPV at different locations. In particular, the data were downloaded from CAMS (Copernicus Atmosphere Monitoring Service, n.d.), one of the freely available databases covering Europe. However, while still of significance, it is known that these databases are still subject to non-negligible uncertainties, which can lead to significant energy yield and cost estimation errors (IEA PVPS Task 13, 2020). In order to provide the most reliable conclusions only, an additional quality filter was introduced to remove any potentially biased result. In particular, the energy yields produced using the CAMS data for the four configurations of FPV (two U-values and two tilt angles) were compared with those produced using data from a second database, the PVGIS-SARAH data (Urraca et al., 2018, 2017). Any location in which the yields returned by the two databases deviated by more than 6.5% for any of the four FPV configurations was discarded. This threshold was selected as it is considered a typical uncertainty in PV yield assessment modelling (IEA PVPS Task 13, 2020). This filter removed 21% of the sites, with the highest errors found in the Alpine regions (Fig. S 1). For this reason, 84% of the locations in Switzerland and 70% of the locations in Austria could not be used in the techno-economic analysis. It should be highlighted that all filtered and unfiltered locations were still taken into account for the capacity analysis in Fig. 2 and for the estimation of the potential contribution of FPV to the EU electricity demand.

2.3. Economical Modelling

The economic performance of FPV and LPV were calculated using the Levelized Cost of Electricity (LCOE). This expresses the cost of producing a kWh of electricity over the system lifetime. It was calculated as follows (Micheli et al., 2020):

$$LCOE = \frac{CAPEX + \sum_{t=1}^{T} \frac{\text{OMEX} \cdot (1-Tx) \cdot (1+r_{om})^t}{(1+d)^t} - \sum_{t=1}^{N_d} \frac{D_n \cdot Tx}{(1+d)^t}}{\sum_{t=1}^{T} \frac{E_t \cdot (1-R_D)^t}{(1+d)^t}} \tag{4}$$

where CAPEX is the capital expenditure (or initial investment cost), T is total number of years of operation (set to 25 years), *OMEX* is the yearly operation and maintenance (O&M) expenditure and r_{om} is the rate at which it varies every year, *d* is the discount rate, *Tx* is the income tax, E_t is the AC energy yield profile, and R_D is the system-level degradation rate. E_t was calculated as yearly average of the daily values in 2010 to 2020. D_n is the annual tax depreciation for the PV plant, which allows recovering part of the investment cost through reduced taxes for a given period of time (N_d). In this work, the same depreciation mechanism used in (Jiménez-Castillo et al., 2020) has been applied to all countries. Depreciation has been modelled as linear and constant over a period (N_d) of 20 years, so that: $\mathrm{D_n} = \frac{\mathrm{CAPEX}}{\mathrm{N_d}} = 5\% \cdot \mathrm{CAPEX}$.

The values of the economic parameters used in the analysis are reported in Table S 1. The typical capital expenditure in each country was sourced from the IRENA Renewable Cost Database (IRENA, 2021). OMEX were also set as in the IRENA Renewable Costs Database, differentiating the countries between the members and the non-members of the Organisation for Economic Co-operation and Development (OECD). r_{om} is set equal to each country's average inflation rate (i) over the 2010 to 2020 period (The World Bank, n.d.). Where not otherwise stated, any missing data was estimated from the values available in nearby countries.

The value of the nominal discount rate, d, was calculated as in (Talavera et al., 2019). The initial investment cost (i.e., CAPEX) can be indeed calculated as:

$$CAPEX = \left(PV_l \cdot \frac{i_l(1-Tx)}{1-\left(1+i_l(1-Tx)\right)^{-N_l}} \cdot \frac{q \cdot \left(1-q^{Nl}\right)}{1-q} \right) + \left((d_s \cdot PV_s) \cdot \frac{q \cdot (1-q^T)}{1-q} + PV_s \cdot q^T \right) \quad (5)$$

where PV_l and PV_s are the capital expenditures financed respectively by loan and equity capital. This work assumes, in agreement with the previous study (Talavera et al., 2019), that 70% of the capital expenditure is financed with a loan and 30% is contributed from equity capital (Justice, 2009). The factor q is related to the nominal discount rate (*d*) through the following equations q=1/(1+d). The loan interest (i_l) and the equity dividends (d_s) are country-specific and their values were set based on the literature found (Table S 1). The loan terms (N_l) was set to 20 years for all the locations of this study. It should be noted that that the left-hand side of equation (5) only equals its right-hand side if the selected value of *d* is equal to the weighted average cost of capital (*WACC*) of the investment.

WACC is the cost that the owner or investor of the project must pay for the use of capital sources in order to finance the investment. Organizations typically use the value of the organization's weighted average cost of capital as nominal discount rate (Short et al., 1995). In this paper, the nominal discount rate was assumed equal to *WACC*.

2.4. Analysis and Mapping

The whole analysis was implemented in Python 3.7. Linear regression was performed through the *linregress* function in the *SciPy* library (Jones et al., 2001). The feature importance analysis was conducted using the extra-tree regressor in the Python's Scikit-learn tool (Pedregosa et al., 2011), fed with normalized values of each variable and default input parameters (i.e. 100 trees, and mean squared error as quality criterion). The analysis was repeated 10 times to evaluate the robustness of the results. The maps were generated using the Cartopy package (Met Office (UK), 2020). Linear interpolation was employed to produce the surface maps from a grid made of the potential FPV locations. The analysis was conducted by taking into account the FPV capacity located in European countries (inclusive of Turkey and part of Russia) in between the 34^{th} and 60^{th} parallels north and in between 10^{th} meridian west and the 45^{th} meridian east.

2.5. Assumption and Limitations

GRanD is the database that reports the largest amount of information for each reservoir, but it might also include only some of the reservoirs present in each country. This is probably affecting the results of the capacity estimation, which should be therefore considered "conservative" (i.e., smaller than the actual potential capacity). In addition, strict filtering criteria sourced from (Spencer et al., 2019) were applied, potentially leading to an additional underestimation of the capacity. The calculation was based on the representative surface area of each reservoir, and it did not take into account the shape of the reservoir or any potential variation that can occur over the time. The land requirement estimation was purely based on an arithmetical calculation (Micheli, 2021), with no minimum spacing set between rows. Since a minimum spacing was set for each tilt angle at each location, the effect of intra-row shading was not considered in the energy yield calculation.

The analysis took into account the reservoirs located within the 45°0'E and 10°0'W meridians, and the 34°0'N and 60°0'N parallels. North African and Middle Eastern countries were not included in the analysis. The maps, the boxplots and the results were generated by modelling LPV and FPV performance on the suitable reservoirs, rather than on a grid. This was done so that the results did not assume a forcedly uniform distribution but could rather represent more realistically the geographical distribution of the FPV capacity in each country. It should be reinstated that the maps were based on the data points that returned acceptable deviations between the energy yields calculated with CAMS and PVGIS-SARAH radiation data.

This work did not consider potential additional costs that FPV might require, during installation (e.g., for submerged cables) or during operation (e.g., increased O&M costs). In addition, both LPV and FPV modules were modeled only as monofacial, fixed and southward oriented tilt systems. The simulation considered a fixed degradation rate, equal for LPV and FPV. This assumption was based on recent experimental works that reported similar rates for FPV and LPV modules in the first years of operation. Indeed, after 17 months of operation, a FPV system in West Bengal, India, showed similar degradation rates than a co-located LPV system (Goswami and Sadhu, 2021). Also the large testbed in Singapore did not show signs of more severe degradation compared to the typical LPV rates after 3 years of operation (Luo et al., 2021).

The 2020 CAPEX for United Kingdom was not available in (IRENA, 2021) and was set equal to the 2019 value reported in (IRENA, 2020).

3. Results and Discussion

The region considered in this study has a significant potential to host floating capacity, with a conservative estimation of almost 22500 km^2 of water surface available. Fig. 2 shows the FPV capacity that each of the investigated countries could host covering 1% of the available water surface. Each percentage point of water surface covered with adequately distanced 10°-tilted modules would add 40 GW of new FPV capacity in the considered region. This would be 36 GW if modules were tilted at 20°. It should be noted that at least 9% of the surface available is made of salt-water (i.e., Lake IJssel in the Netherlands), potentially exposing FPV to harsher conditions than fresh water (Hooper et al., 2021).

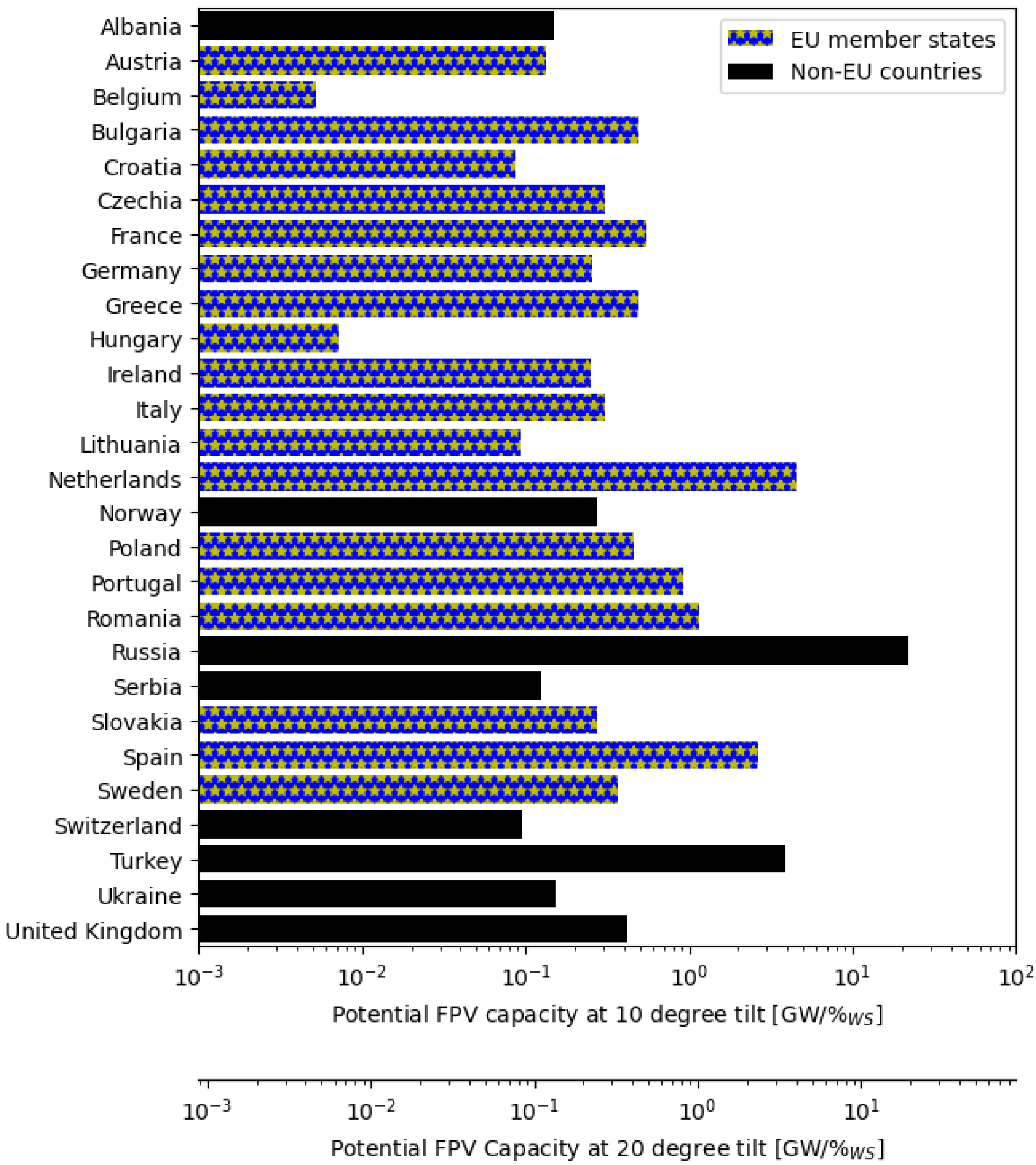

Fig. 2. Potential FPV capacity per country, assuming water surface coverage of 1%. EU and non-EU countries are colored differently. The investigated area is in between the 34th and the 60th parallels north, and the 10th meridian west and the 45th meridian east. The 10-degree capacity is 13% larger than the 20-degree capacity, thanks to the reduced spacing needed in between rows to avoid mutual shading.

A third of the continental water surface is located in EU member states, which could host 13 GW/%$_{WS}$ and 12 GW/%$_{WS}$ (Fig. 2) at 10° and 20° tilt respectively. It should be noted that each percentage point of reservoir surface covered by PV modules would increase the EU PV capacity by 10 to 11% compared to the 2019 value. In addition, it could contribute to achieving 6 to 9% of European 2030 goals for PV. This new capacity is expected to generate ˜16 TWh/year/%$_{WS}$ within the EU, contributing to the 0.5%/%$_{WS}$ of the current electricity demand.

The capacity is not uniformly distributed among the EU member states, which also have dissimilar ambitions in their PV capacity targets (Fig. 3). This means that FPV can contribute differently to the national 2030 goals of the various EU members. Slovakia, Romania, and Bulgaria are the countries that can benefit the most of FPV, as even small percentages of water coverage can substantially contribute towards their 2030 goals. However, they represent less than 5% of the additional PV capacity planned by the EU members as a whole. There are also several countries in which each percentage point of water surface covered with modules can contribute to achieving more than 10% of the national 2030 goals. These countries represent in between 17 and 39% of the EU goals. However, it should be noted that, even where the contribution might seem limited, FPV can still have a significant effect. This is the case of Spain, where, for example, each percentage point of water surface could contribute to 7-8% of the PV capacity goals, providing one of the largest absolute additions in terms of GW/$\%_{ws}$ (Fig. 2).

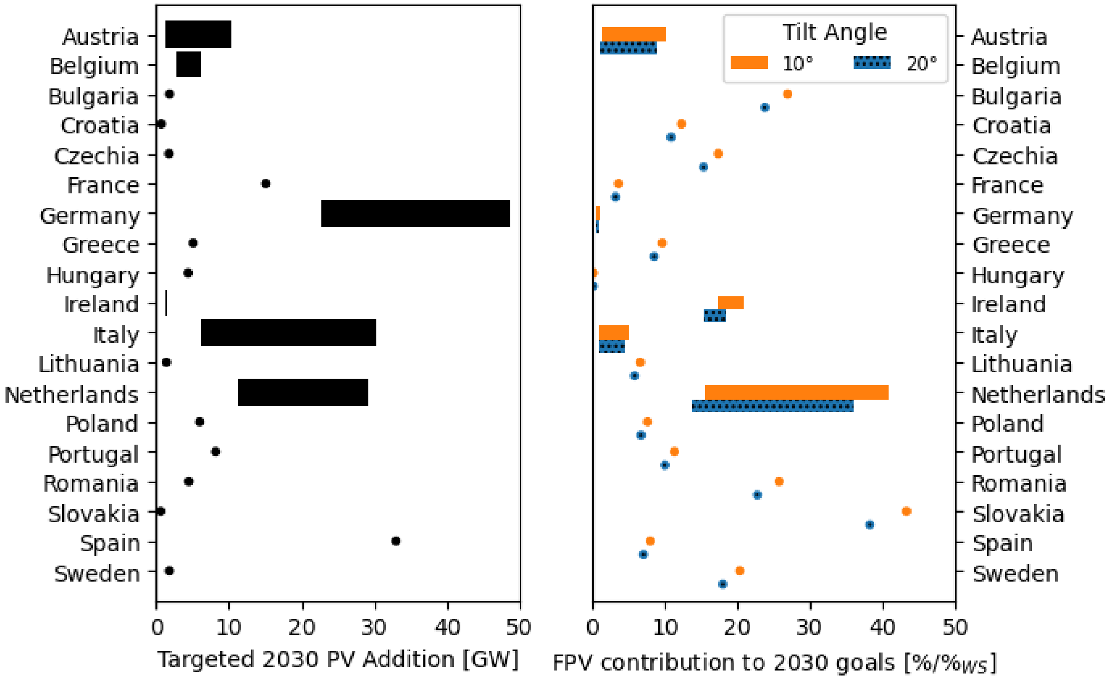

Fig. 3. Left: additional PV capacity to be added in between 2020 and 2030. Right: Potential contribution of FPV to 2030 PV targets, per unit of water surface. Bars are shown if there targets for high and low scenarios are reported (i.e., Austria, Belgium, Germany, Italy, Luxembourg, and Netherlands). In the other cases, only one target is set, and round markers are used.

Because of the higher thermal exchange and the lower tilts angles, the difference in energy yield between FPV and LPV changes depending on both the modelled scenario and the location (Fig. 4). Overall, as expected, the better the FPV thermal performance, the better its electrical performance. Indeed, the most optimistic scenario (A) returns yields up to 2% higher for FPV than LPV. In this scenario, 20-degree tilt FPV grants higher yields than optimally tilted LPV in several countries (Fig. S 3). In other configurations and scenarios, however, the yields of FPV are typically lower than that of LPV, especially at 10-degree tilt. These results highlight that the effect of the tilt angle on the energy conversion is significant. Therefore, in order to fairly compare FPV and LPV for utility-scale purposes, the different thermal behaviors and the different tilt or tracking configurations should be both taken into account.

In general, FPV is found to have the best performance compared to LPV in the southernmost countries (Fig. S 3). On the other hand, the worst performances are found in the northern countries and in the alpine region. However, the results of each scenario could vary significantly even within the borders of a country. This is the case of Italy, for example, where FPV is expected to perform significantly better in the south, compared to the mountainous areas in the north.

These results are explained by the fact that the ratio between the direct irradiances on the normal and the horizontal planes (DNI to BHI ratio) dominates the difference in yields between FPV and LPV (Fig. S 4). This ratio is related to the average elevation of the sun: the higher its value, the lower the angular and reflection losses for low-tilt FPV modules compared to optimally tilted LPV system. In addition, one can expect that the better heat transfer modelled in most scenarios would also favor the deployment of FPV in the southern and warmer areas of the continents. For this reason, the average ambient temperature is found to be the second most important parameter and the alpine region seems to experience lower FPV performance compared to surrounding areas of similar latitude.

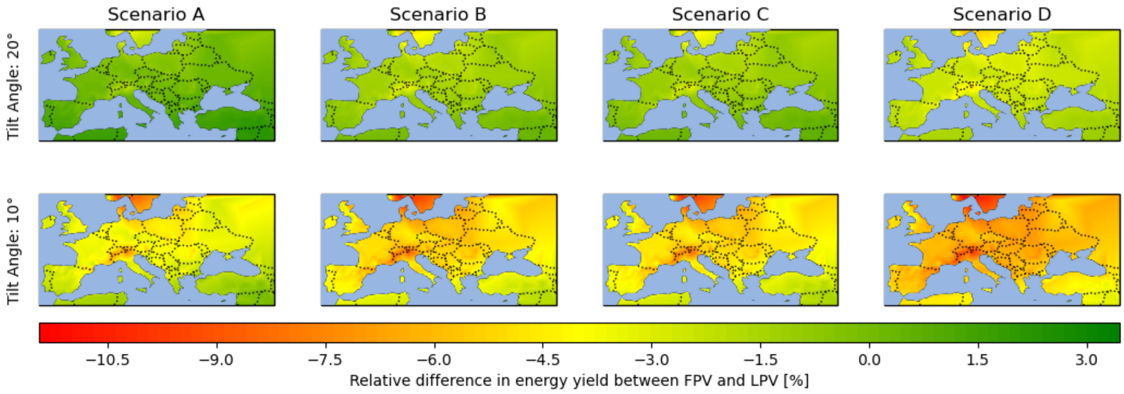

Fig. 4. Energy yield gains of FPV compared to LPV, i.e., relative difference between the energy yields of FPV and LPV, in the various scenarios. Positive values mean that FPV over-perform optimally tilted LPV.

The different yields found for FPV and LPV translate in different CAPEX allowances if FPV want to be cost competitive with LPV (Fig. 5). The relative variations in CAPEX allowances for FPV follow, for most countries, a trend similar to that of the relative variation of energy yield (Fig. S 5 and Fig. S 3). The same factors that dominate the energy yield are also found to have the biggest influence on the economic performance of FPV. However, countries with higher LPV CAPEX (Table S 1) penalize systems that have limited yields, allowing lower CAPEX. This is the reason why Russia, which has the highest LPV CAPEX among the investigated countries, experiences the minimum absolute CAPEX allowance for FPV in scenario D (Fig. 5). Indeed, each missed kWh of energy in Russia has a higher economic value from an LCOE perspective, because of the greater initial investment.

In line with the previous finding, northern and alpine countries are still those less favorable for FPV. These, unfortunately, are even the countries in which additional CAPEX expenses can be expected to strengthen the buoyancy systems in order to support heavy snow loads (Bellini, 2021).

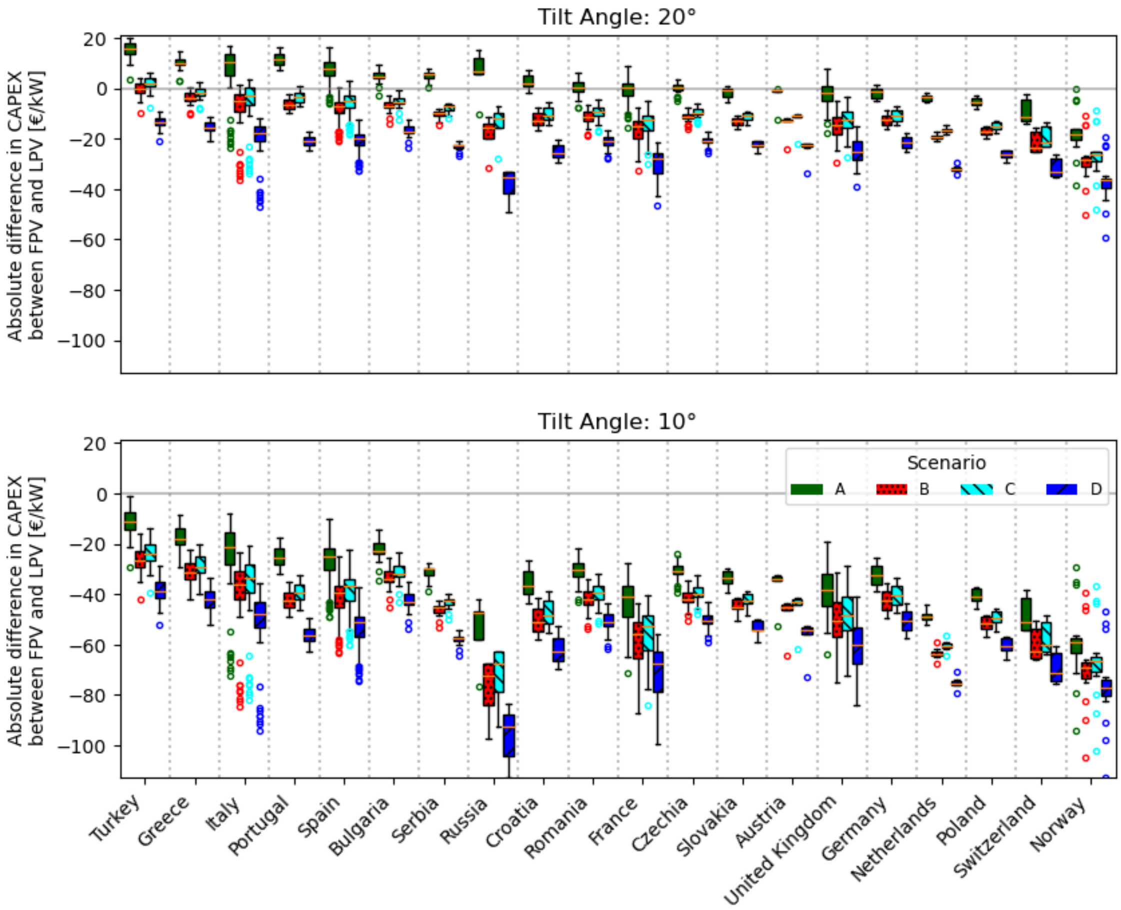

Fig. 5. Absolute difference between the targeted CAPEX for FPV and the LPV CAPEX. Negative values indicate that $CAPEX_{FPV}$ should be lower than $CAPEX_{LPV}$. The boxplot does not include countries with less than 5 data points. Countries are ordered as in Fig. S 3.

Several authors expect that a fully developed FPV industry would be able to cut some of the capital expenditures compared to traditional PV. Indeed, the installation of FPV does not require major site preparation works, such as leveling or the laying of foundations (World Bank Group et al., 2018). However, currently, the cost of floaters still has a significant weight in the FPV economics (World Bank Group et al., 2018), but this is expected to decrease significantly in future. The easier installation and the low-cost floaters would reduce the “Racking and mounting” costs, which, in 2020, represented on average the 10% of the LPV CAPEX in the investigated countries (IRENA, 2021). Ideally, if these costs could be eliminated thanks to easier installation and cheaper floaters, FPV would become more cost competitive than LPV in most of the countries in all four scenarios (Fig. 6).

In addition, the hybridization with hydropower could potentially cut the grid connection costs, as FPV could make use, in this case, of existing electric infrastructures (Fang et al., 2017). In 2020, these costs represented 8% of the CAPEX of PV (IRENA, 2021). Removing both these costs would make FPV cost competitive also in the rest of the countries in all the modelled scenarios (Fig. 6).

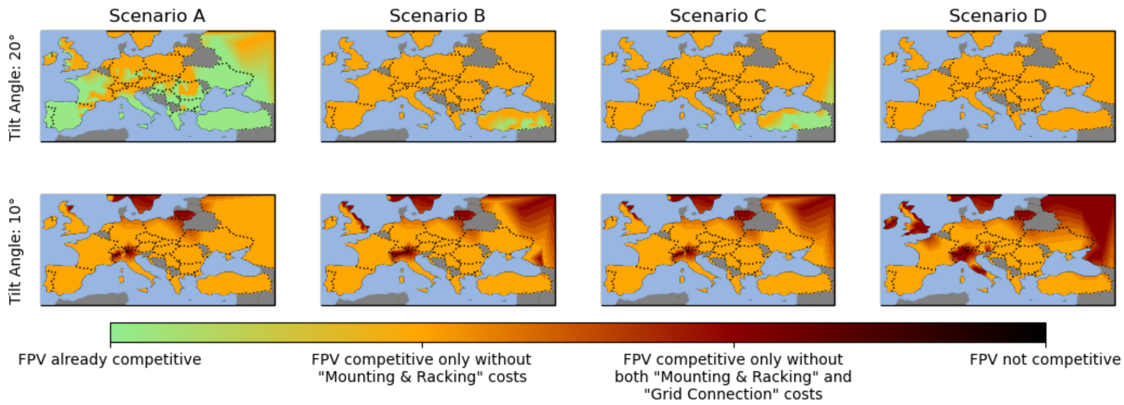

Fig. 6. Areas of competiveness for FPV, depending on CAPEX cost reductions. Countries in grey are not included in the analysis.

So far, the analysis has not taken into account the cost of land. Lower rent fees have been reported for water compared to land, because water surfaces are not of value for other activities, such as agriculture or construction (Gorjian et al., 2021). As already discussed in (Micheli, 2021), lower annual rents could positively affect LCOE of FPV and therefore contribute to its deployment. In addition, one should take into account that, because of the row spacing needed for tilted modules, FPV will also have higher power densities than optimally tilted PV systems. According to eq. (1), optimally tilted LPV modules occupy on average 7.0 m^2/kW, whereas FPV would occupy 6.3 and 5.5 m^2/kW at 20- and 10-degree tilt respectively. This means that FPV will occupy less land per unit of kW installed and, therefore, even for the same cost per m^2, will have lower rent fees per kW (Fig. S 7).

The reduced spacing in this case also leads to higher energy densities for FPV. These, indeed, are estimated to range from 202 to 223 kWh/m^2/year, depending on tilt angle and scenario, compared to the 185-188 kWh/m^2/year of LPV. Therefore, despite the lower yields, low tilt FPVs are expected to be more appealable in areas where land has high monetary or ecological value.

On the other hand, the significant impact of the module's inclination on the results can push FPV designers and installers to maximize the tilt angle of their systems. However, higher tilt angles are likely to require additional expenditures to strengthen the FPV foundations in order to face stronger wind loads (Silvério et al., 2018). The difference in CAPEX between FPV and LPV varies with the FPV tilt angle, following a parabolic trend (Fig. S 8). However, the correlation between CAPEX and tilt angle can be modelled as a straight line at the low tilt angles typical in FPV (≤20°). The slopes of these approximated lines are shown in Fig. 7; they express the increase in CAPEX that FPV can face thanks to the additional energy it would produce at higher tilt angles. These represent the extra funds that could be ideally invested to strengthen the FPV foundation. Even in this case, the results strongly depend on the location. The highest benefits, in terms of relative increase, are found in the Alps and in the Scandinavian countries (left plot of Fig. 7), areas where the potential improved FPV cooling is not significantly advantageous. On the other hand, the absolute gain in CAPEX per unit of tilt angle (right plot of Fig. 7) strongly depends on the LPV CAPEX. For this reason, the highest absolute values are found in Russia, a country whose CAPEX is almost twice than that of any other country.

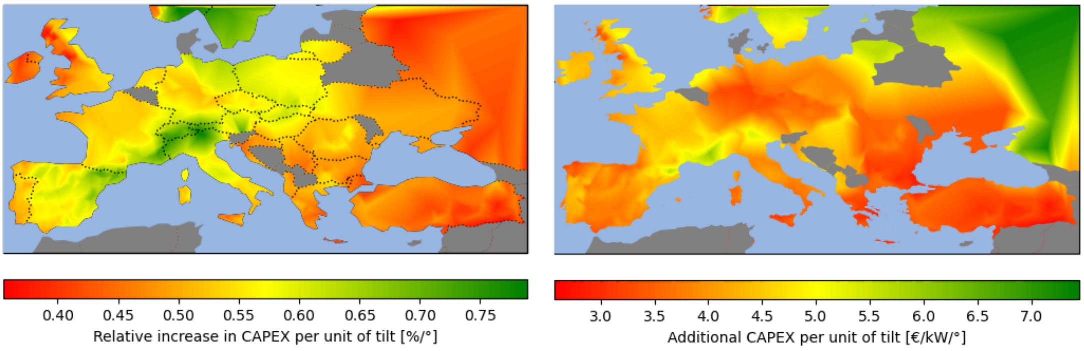

Fig. 7. Increase in allowed CAPEX per unit of tilt to match the LCOE of LPV: relative value on the left and absolute value on the right. The linear fit is valid for tilt angles in between 5 and 20 degrees. Countries not included in the analysis are colored in grey.

In addition to the tilt angle, also the albedo has typically a lower value in FPV installations compared to LPV due to the low reflectance of water (Liu et al., 2018). Despite the expectations, this can have a significant effect even when the employed modules are monofacial. Indeed, even if mounted at optimum tilts, FPV would not overperform LPV in many sites if its albedo is not raised (Fig. S 9). If FPV modules had the same optimal inclination and the same thermal performance (Scenario D) of LPV, FPV would still underperform by 1.3% on average compared to LPV because of the difference in albedo. Previous authors have suggested installing reflectors on floaters to favor the deployment of bifacial modules on water (Ziar et al., 2021). This solution could be applied also to monofacial systems, even if the effect of the floater's design on the thermal exchange of FPV is still being investigated and raising the irradiance on the back surface could also increase the PV modules' temperature. Fig. 8 shows the economic value of each gained point of albedo in the various modelled FPV configurations. Raising the FPV albedo by 0.01 is found to lead to increases in CAPEX of at least 0.05 €/kW per point of albedo at tilts of 10° or higher. As expected, however, these benefits are even greater if FPV modules are installed at higher tilt angles. Also in this case, Russia is the country benefitting the most of higher albedos because of the higher CAPEX.

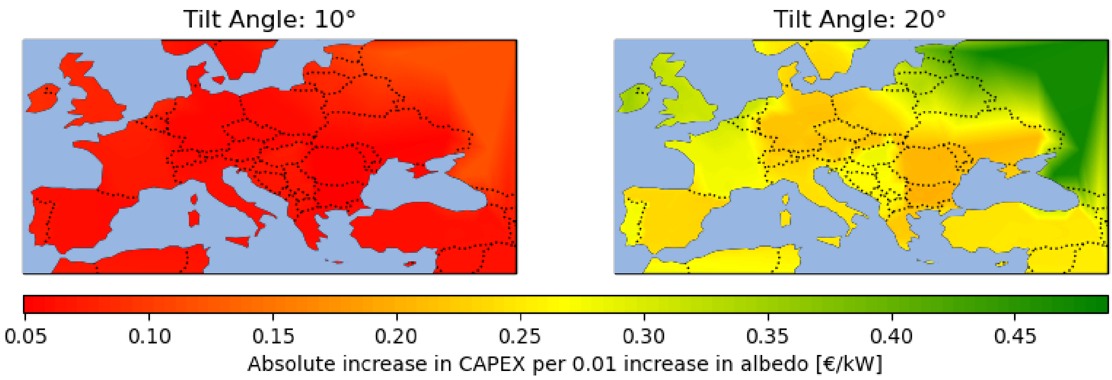

Fig. 8. Average increase in FPV CAPEX per point of albedo (i.e., to increase the albedo by 0.01). The data are obtained as average of the four scenarios. The thermal effect of the increased irradiance on the back surface of the monofacial module is not taken into account.

This work presents an assessment of air-cooled systems, the most common FPV configuration so far. It shows that the thermal management of floating modules is key for the success and cost-competitivity of FPV. For this reason, the thermal benefits of additional configurations (i.e., water-cooled FPV modules) should also be investigated in future. These can be, for example, horizontal modules directly in contact with the water surface, which have been found to achieve even higher U-values and lower temperatures than air-cooled FPV (Kjeldstad et al., 2021). Moreover, partially submerged FPV modules have also the opportunity to improve the heat transfer, as experimentally demonstrated by (Elminshawy et al., 2022). Their analysis, however, will require access to additional data, such as the water body temperatures. The employment of different databases to model the various modules' configurations will require additional calibration and validation steps, in order to avoid biases in the results due to the intrinsic differences of the data sources.

Other factors can impact the cost-competitiveness of FPV, in addition to the cooling mechanisms. These should also be taken in account in future. For example, the present analysis has considered the same O&M costs for LPV and FPV. However, dissimilar O&M costs would influence the cost-competitiveness of FPV. A previous review (Sahu et al., 2016) suggested that the O&M costs of FPV could be even lower than LPV, because of the limited dust soiling and of the immediate and free availability of water. However, a subsequent review (Gorjian et al., 2021) has highlighted that O&M operations might actually be more expensive in FPV because of the need of water vehicles or underwater operations. As more field data become available, future studies should take into account potential dissimilarities in O&M costs between FPV and LPV. Additionally, differences in factors such as degradation, bifaciality, and/or water savings should also be considered in future FPV cost assessments.

4. Conclusions

This work investigates the potential and the economic viability of floating photovoltaics (FPV) in Europe. The analysis makes use of referenced parameters and models and of satellite-derived data specific to each suitable water basin to estimate the capacity, the cell temperature, the energy yields, and the costs of FPV and LPV systems. The results show that FPV could contribute substantially to the achievement of the 2030 targets set by the EU, preventing conflicts with agriculture and risks for biodiversity. If the expected lower operating temperatures were confirmed, FPV could even over-perform traditional land-based PV (LPV) in the southernmost countries of the continent in terms of energy yield. A specific analysis shows that this result is motivated by (i) the higher Sun elevations and (ii) the higher temperatures occurring in these countries. The first factor reduces the angular and reflection losses in low-tilt FPV, whereas the second one favors FPV when it experiences better cooling compared to LPV and it is therefore strictly dependent on the thermal behavior of the system.

In addition to the reduced land occupancy, FPV is expected to require in future lower capital costs than LPV. This can favor its deployment even in conditions of lower yields. The FPV cost of electricity is indeed found to be as low as that of LPV if the "Racking and Mounting" and/or the "Grid Connection" costs are eliminated thanks to the easier installation and the use of pre-existing electrical infrastructures. Moreover, the investigation shows that factors such as the tilt angles and the albedo, whose values are typically low in FPV applications, seriously affect the FPV performance. The present work assesses the economic impact of these variables and identifies the capital expenditures that FPV owners and designers can invest to increase their values. It is found that each additional degree of tilt angle in FPV installations is worth between 2.5 and 7.5 €/kW of capital expenditure, with the highest values in Russia, and the lowest in the Alpine and Scandinavian regions.

Acknowledgments

L. Micheli's work was supported by the Spanish Ministry of Science and Innovation under the Ramón y Cajal 2020 program (RYC2020-030094-I) and by Sole4PV, a project funded by the Italian Ministry of University and Research under the 2019 «Rita Levi Montalcini» Program for Young Researchers. E.F. Fernández thanks the Spanish Ministry of Science, Innovation and Universities for the funds received under the "Ramón y Cajal Programme" (RYC-2017-21910).

Data availability

The economic data used in this analysis are provided in the Supplemental Information. The code for the calculation of the capacity, energy yields and the LCOE will be made available on GitHub.

CRediT authorship contribution statement

Leonardo Micheli: Conceptualization, Methodology, Data Curation, Software, Investigation, Formal analysis, Validation, Visualization, Writing – Original Draft. **Diego L. Talavera**: Methodology, Data Curation, Validation, Writing – Review & Editing. **Marco Giuseppe Tina**: Methodology, Writing – Review & Editing. **Florencia Almonacid**: Methodology, Validation, Writing – Review & Editing. **Eduardo F. Fernandez**: Methodology, Validation, Writing – Review & Editing.

Declaration of competing interest

The authors declare that they have no known competing financial interests or personal relationships that could have appeared to influence the work reported in this paper.

References

Álvarez, C., Zafra, M., 2021. Cuánto ocupan las megacentrales solares: investigadores alertan del impacto del 'boom' fotovoltaico. El Pais.

Bellini, E., 2021. What happens to floating PV when the water surface freezes? [WWW Document]. pv-magazine. URL https://www.pv-magazine.com/2021/01/15/what-happens-to-floating-pv-when-the-water-surface-freezes/ (accessed 9.27.21).

Bontempo Scavo, F., Tina, G.M., Gagliano, A., Nižetić, S., 2021. An assessment study of evaporation rate models on a water basin with floating photovoltaic plants. Int. J. Energy Res. 45, 167–188. https://doi.org/10.1002/er.5170

Copernicus Atmosphere Monitoring Service, n.d. CAMS solar radiation time-series [WWW Document]. URL https://ads.atmosphere.copernicus.eu/ (accessed 11.9.20).

Cromratie Clemons, S.K., Salloum, C.R., Herdegen, K.G., Kamens, R.M., Gheewala, S.H., 2021. Life cycle assessment of a floating photovoltaic system and feasibility for application in Thailand. Renew. Energy 168, 448–462. https://doi.org/10.1016/j.renene.2020.12.082

De Soto, W., Klein, S.A., Beckman, W.A., 2006. Improvement and validation of a model for photovoltaic array performance. Sol. Energy 80, 78–88. https://doi.org/10.1016/j.solener.2005.06.010

Department of Economic and Social Affairs, 2016. The Sustainable Development Goals Report. New York, NY. https://doi.org/10.1177/000331979004100307

Dimson, E., Marsh, P., Staunton, M., 2011. Equity Premia Around the World. SSRN.

https://doi.org/10.2139/ssrn.1940165

Dobos, A.P., 2014. PVWatts Version 5 Manual.

Dörenkämper, M., Wahed, A., Kumar, A., de Jong, M., Kroon, J., Reindl, T., 2021. The cooling effect of floating PV in two different climate zones: A comparison of field test data from the Netherlands and Singapore. Sol. Energy 219, 15–23. https://doi.org/10.1016/j.solener.2021.03.051

El Hammoumi, A., Chalh, A., Allouhi, A., Motahhir, S., El Ghzizal, A., Derouich, A., 2021. Design and construction of a test bench to investigate the potential of floating PV systems. J. Clean. Prod. 278, 123917. https://doi.org/10.1016/j.jclepro.2020.123917

Elminshawy, N.A.S., Osama, A., Saif, A.M., Tina, G.M., 2022. Thermo-electrical performance assessment of a partially submerged floating photovoltaic system. Energy 123444. https://doi.org/10.1016/j.energy.2022.123444

European Central Bank, n.d. Euro foreign exchange reference rates [WWW Document]. URL https://www.ecb.europa.eu/stats/policy_and_exchange_rates/euro_reference_exchange_rates/html/eurofxref-graph-usd.en.html (accessed 9.24.21).

Faiman, D., 2008. Assessing the outdoor operating temperature of photovoltaic modules. Prog. Photovoltaics Res. Appl. 16, 307–315. https://doi.org/10.1002/pip.813

Fang, W., Huang, Q., Huang, S., Yang, J., Meng, E., Li, Y., 2017. Optimal sizing of utility-scale photovoltaic power generation complementarily operating with hydropower: A case study of the world's largest hydro-photovoltaic plant. Energy Convers. Manag. 136, 161–172. https://doi.org/10.1016/j.enconman.2017.01.012

Gonzalez Sanchez, R., Kougias, I., Moner-Girona, M., Fahl, F., Jäger-Waldau, A., 2021. Assessment of floating solar photovoltaics potential in existing hydropower reservoirs in Africa. Renew. Energy 169, 687–699. https://doi.org/10.1016/j.renene.2021.01.041

Gorjian, S., Sharon, H., Ebadi, H., Kant, K., Scavo, F.B., Tina, G.M., 2021. Recent technical advancements, economics and environmental impacts of floating photovoltaic solar energy conversion systems. J. Clean. Prod. 278, 124285. https://doi.org/10.1016/j.jclepro.2020.124285

Goswami, A., Sadhu, P.K., 2021. Degradation analysis and the impacts on feasibility study of floating solar photovoltaic systems. Sustain. Energy, Grids Networks 26, 100425. https://doi.org/10.1016/j.segan.2020.100425

Gschwind, B., Wald, L., Blanc, P., Schroedter-homscheidt, M., Arola, A., 2019. Improving the McClear model estimating the downwelling solar radiation at ground level in cloud-free conditions –. Meteorol. Zeitschrift 28, 147–163. https://doi.org/10.1127/metz/2019/0946

Gueymard, C., 1993. Critical analysis and performance assessment of clear sky solar irradiance models using theoretical and measured data. Sol. Energy 51, 121–138. https://doi.org/10.1016/0038-092X(93)90074-X

Haugwitz, F., 2020. Floating solar PV gains global momentum. PV Mag. Int. 1–10.

Hersbach, H., Bell, B., Berrisford, P., Biavati, G., Horányi, A., Muñoz Sabater, J., Nicolas, J., Peubey, C., Radu, R., Rozum, I., Schepers, D., Simmons, A., Soci, C., Dee, D., Thépaut, J.-N., 2018. ERA5 hourly data on single levels from 1979 to present [WWW Document]. Copernicus Clim. Chang. Serv. Clim. Data Store. URL 10.24381/cds.adbb2d47 (accessed

9.13.21).

Holmgren, W.F., Hansen, C.W., Mikofski, M.A., 2018. pvlib python: a python package for modeling solar energy systems. J. Open Source Softw. 3. https://doi.org/https://doi.org/10.21105/joss.00884

Hooper, T., Armstrong, A., Vlaswinkel, B., 2021. Environmental impacts and benefits of marine floating solar. Sol. Energy 219, 11–14. https://doi.org/10.1016/j.solener.2020.10.010

IEA PVPS Task 13, 2020. Uncertainties in Yield Assessments and PV LCOE.

International Renewable Energy Agency, 2019. RENEWABLE POWER GENERATION COSTS IN 2019.

IRENA, 2021. Renewable Power Generation Costs in 2020. Abu Dhabi.

IRENA, 2020. Renewable Power Generation Costs in 2019. Abu Dhabi.

Jiménez-Castillo, G., Muñoz-Rodriguez, F.J., Rus-Casas, C., Talavera, D.L., 2020. A new approach based on economic profitability to sizing the photovoltaic generator in self-consumption systems without storage. Renew. Energy 148, 1017–1033. https://doi.org/10.1016/j.renene.2019.10.086

Jones, E., Oliphant, E., Peterson, P., et al., 2001. SciPy: Open Source Scientific Tools for Python.

Justice, S., 2009. Private Financing of Renewable Energy. A guide for Policy makers, UNEP; SEFI; New Energy Finance; Chatham House.

Kasten, F., Young, A.T., 1989. Revised optical air mass tables and approximation formula. Appl. Opt. 28, 4735–4738. https://doi.org/10.1364/AO.28.004735

Kjeldstad, T., Lindholm, D., Marstein, E., Selj, J., 2021. Cooling of floating photovoltaics and the importance of water temperature. Sol. Energy 218, 544–551. https://doi.org/10.1016/j.solener.2021.03.022

Kougias, I., Taylor, N., Kakoulaki, G., Jäger-Waldau, A., 2021. The role of photovoltaics for the European Green Deal and the recovery plan. Renew. Sustain. Energy Rev. 144, 111017. https://doi.org/10.1016/j.rser.2021.111017

KPMG, n.d. Corporate Tax Rates Table [WWW Document]. URL https://home.kpmg/xx/en/home/services/tax/tax-tools-and-resources/tax-rates-online/corporate-tax-rates-table.html (accessed 9.21.21).

Kumar, M., Niyaz, H.M., Gupta, R., Mohammed Niyaz, H., Gupta, R., 2021. Challenges and opportunities towards the development of floating photovoltaic systems. Sol. Energy Mater. Sol. Cells 233, 111408. https://doi.org/10.1016/j.solmat.2021.111408

Lee, N., Grunwald, U., Rosenlieb, E., Mirletz, H., Aznar, A., Spencer, R., Cox, S., 2020. Hybrid floating solar photovoltaics-hydropower systems: Benefits and global assessment of technical potential. Renew. Energy 162, 1415–1427. https://doi.org/10.1016/j.renene.2020.08.080

Lefèvre, M., Oumbe, A., Blanc, P., Espinar, B., Gschwind, B., Qu, Z., Wald, L., Schroedter-Homscheidt, M., Hoyer-Klick, C., Arola, A., Benedetti, A., Kaiser, J.W., Morcrette, J.J., 2013. McClear: A new model estimating downwelling solar radiation at ground level in clear-sky conditions. Atmos. Meas. Tech. 6, 2403–2418. https://doi.org/10.5194/amt-6-2403-2013

Lehner, B., Liermann, C.R., Revenga, C., Vörömsmarty, C., Fekete, B., Crouzet, P., Döll, P., Endejan, M., Frenken, K., Magome, J., Nilsson, C., Robertson, J.C., Rödel, R., Sindorf, N., Wisser, D., 2011. High-resolution mapping of the world's reservoirs and dams for sustainable river-flow management. Front. Ecol. Environ. https://doi.org/10.1890/100125

Lindholm, D., Kjeldstad, T., Fjær, H.G., 2021. Heat loss coefficients computed for floating PV modules. Prog. Photovoltaics Res. Appl. 29. https://doi.org/10.1002/pip.3451

Liu, H., Krishna, V., Lun Leung, J., Reindl, T., Zhao, L., 2018. Field experience and performance analysis of floating PV technologies in the tropics. Prog. Photovoltaics Res. Appl. 26, 957–967. https://doi.org/10.1002/pip.3039

Loutzenhiser, P.G., Manz, H., Felsmann, C., Strachan, P.A., Frank, T., Maxwell, G.M., 2007. Empirical validation of models to compute solar irradiance on inclined surfaces for building energy simulation. Sol. Energy 81, 254–267. https://doi.org/10.1016/j.solener.2006.03.009

Luo, W., Isukapalli, S.N., Vinayagam, L., Ting, S.A., Pravettoni, M., Reindl, T., Kumar, A., 2021. Performance loss rates of floating photovoltaic installations in the tropics. Sol. Energy 219, 58–64. https://doi.org/10.1016/j.solener.2020.12.019

Marino, A., 2021. The "Do No Significant Harm" principle [WWW Document]. URL https://ec.europa.eu/info/funding-tenders/opportunities/docs/2021-2027/horizon/other/events/20210421/do-no-significant-harm_en.pptx (accessed 10.20.21).

Marion, B., Adelstein, J., Hadyen, H., Hammond, B., Flecther, T., 2005. Performance parameters for grid-connected PV systems, in: 31st IEEE Photovoltaics Specialists Conference and Exhibition. pp. 1601–1606.

Met Office (UK), 2020. Cartopy v0.11.2. 22 [WWW Document]. URL https://github.com/SciTools/cartopy/archive/v0.11.2.tar.gz%0A (accessed 4.21.21).

Micheli, L., 2021. Energy and economic assessment of floating photovoltaics in Spanish reservoirs: cost competitiveness and the role of temperature. Sol. Energy 227, 625–634. https://doi.org/10.1016/j.solener.2021.08.058

Micheli, L., Theristis, M., Talavera, D.L., Almonacid, F., Stein, J.S., Fernández, E.F., 2020. Photovoltaic cleaning frequency optimization under different degradation rate patterns. Renew. Energy 166, 136–146. https://doi.org/10.1016/j.renene.2020.11.044

Padilha Campos Lopes, M., de Andrade Neto, S., Alves Castelo Branco, D., Vasconcelos de Freitas, M.A., da Silva Fidelis, N., 2020. Water-energy nexus: Floating photovoltaic systems promoting water security and energy generation in the semiarid region of Brazil. J. Clean. Prod. 273. https://doi.org/10.1016/j.jclepro.2020.122010

Pedregosa, F., Varoquaux, G., Gramfort, A., Michel, V., Thirion, B., Grisel, O., Blondel, M., Prettenhofer, P., Weiss, R., Dubourg, V., Vanderplas, J., Passos, A., Cournapeau, D., Brucher, M., Perrot, M., Duchesnay, E., 2011. Scikit-learn: Machine Learning in Python. J. ofMachine Learn. Res. 12, 2825–2830.

Perez, R., Ineichen, P., Seals, R., Michalsky, J., Stewart, R., 1990. Modeling daylight availability and irradiance components from direct and global irradiance. Sol. Energy 44, 271–289.

Perez, R., Seals, R., Ineichen, P., Geneve, U. De, Appliquee, G.D.P., Stewartt, R., 1987. A new simplified version of the Perez diffuse irradiance model for tilted surfaces. Sol. Energy 39, 221–231.

Perez, R., Stewart, R., Seals, R., Guertin, T., 1988. The Development and Verification of the Perez Diffuse Radiation Model. Albuquerque, New Mexico.

Peters, I.M., Nobre, A.M., 2020. On Module Temperature in Floating PV Systems, in: 2020 47th IEEE Photovoltaic Specialists Conference (PVSC). IEEE, pp. 0238–0241. https://doi.org/10.1109/PVSC45281.2020.9300426

Peters, I.M.M., Nobre, A.M.M., 2022. Deciphering the thermal behavior of floating photovoltaic installations. Sol. Energy Adv. 2, 100007. https://doi.org/10.1016/j.seja.2021.100007

PVsyst SA, n.d. PVsyst [WWW Document]. URL https://www.pvsyst.com/ (accessed 5.6.21).

Qu, Z., Oumbe, A., Blanc, P., Espinar, B., Gesell, G., Gschwind, B., Klüser, L., Lefèvre, M., Saboret, L., Schroedter-Homscheidt, M., Wald, L., 2017. Fast radiative transfer parameterisation for assessing the surface solar irradiance: The Heliosat-4 method. Meteorol. Zeitschrift 26, 33–57. https://doi.org/10.1127/metz/2016/0781

Rehbein, J.A., Watson, J.E.M., Lane, J.L., Sonter, L.J., Venter, O., Atkinson, S.C., Allan, J.R., 2020. Renewable energy development threatens many globally important biodiversity areas. Glob. Chang. Biol. 26, 3040–3051. https://doi.org/10.1111/gcb.15067

Rosa-Clot, M., Tina, G.M., 2020. Current status of FPV and trends, Floating PV Plants. Elsevier Inc. https://doi.org/10.1016/B978-0-12-817061-8.00002-6

Sahu, A., Yadav, N., Sudhakar, K., 2016. Floating photovoltaic power plant: A review. Renew. Sustain. Energy Rev. 66, 815–824. https://doi.org/10.1016/j.rser.2016.08.051

Serrano, D., Margalida, A., Pérez-García, J.M., Juste, J., Traba, J., Valera, F., Carrete, M., Aihartza, J., Real, J., Mañosa, S., Flaquer, C., Garin, I., Morales, M.B., Alcalde, J.T., Arroyo, B., Sánchez-Zapata, J.A., Blanco, G., Negro, J.J., Tella, J.L., Ibañez, C., Tellería, J.L., Hiraldo, F., Donázar, J.A., 2020. Renewables in Spain threaten biodiversity. Science (80-.). 370, 1182–1183. https://doi.org/10.1126/science.abf6509

Short, W., Packey, D.J., Holt, T., 1995. A manual for the Economic Evaluation of Energy Efficiency and Renewable Energy Technologies, NREL/TP-462-5173. National Renewable Energy Laboratory, Golden, Colorado (USA).

Silvério, N.M., Barros, R.M., Tiago Filho, G.L., Redón-Santafé, M., Santos, I.F.S. dos, Valério, V.E. de M., 2018. Use of floating PV plants for coordinated operation with hydropower plants: Case study of the hydroelectric plants of the São Francisco River basin. Energy Convers. Manag. 171, 339–349. https://doi.org/10.1016/j.enconman.2018.05.095

SolarPower Europe, 2020. Global Market Outlook For Solar Power 2020-2024.

Späth, L., 2018. Large-scale photovoltaics? Yes please, but not like this! Insights on different perspectives underlying the trade-off between land use and renewable electricity development. Energy Policy 122, 429–437. https://doi.org/10.1016/j.enpol.2018.07.029

Spencer, R.S., Macknick, J., Aznar, A., Warren, A., Reese, M.O., 2019. Floating Photovoltaic Systems: Assessing the Technical Potential of Photovoltaic Systems on Man-Made Water Bodies in the Continental United States. Environ. Sci. Technol. 53, 1680–1689. https://doi.org/10.1021/acs.est.8b04735

Talavera, D.L., Muñoz-Cerón, E., Ferrer-Rodríguez, J.P., Pérez-Higueras, P.J., 2019. Assessment of cost-competitiveness and profitability of fixed and tracking photovoltaic systems: The case of five specific sites. Renew. Energy 134, 902–913.

https://doi.org/10.1016/j.renene.2018.11.091

The World Bank, n.d. Inflation, consumer prices (annual %) [WWW Document]. URL https://data.worldbank.org/indicator/FP.CPI.TOTL.ZG?locations=AE. (accessed 11.17.21a).

The World Bank, n.d. World Development Indicators [WWW Document]. URL https://databank.bancomundial.org/reports.aspx?source=2&series=FR.INR.LEND&country= (accessed 9.17.21b).

Trading Economics, 2018. Spain - Lending interest rate [WWW Document].

Trading Economics, n.d. List of Countries by Corporate Tax Rate [WWW Document]. URL https://tradingeconomics.com/country-list/corporate-tax-rate (accessed 9.17.21).

Trina, 2021. Vertex TSM-DE20 585-605W.

Urraca, R., Gracia-amillo, A.M., Koubli, E., Huld, T., Trentmann, J., Riihelä, A., Lindfors, A. V, Palmer, D., Gottschalg, R., Antonanzas-torres, F., 2017. Remote Sensing of Environment Extensive validation of CM SAF surface radiation products over Europe. Remote Sens. Environ. 199, 171–186. https://doi.org/10.1016/j.rse.2017.07.013

Urraca, R., Huld, T., Gracia-amillo, A., Martinez-de-pison, F.J., Kaspar, F., Sanz-garcia, A., 2018. Evaluation of global horizontal irradiance estimates from ERA5 and COSMO-REA6 reanalyses using ground and satellite-based data. Sol. Energy 164, 339–354. https://doi.org/10.1016/j.solener.2018.02.059

World Bank Group, ESMAP, SERIS, 2018. Where Sun Meets Water: Floating Solar Market Report—Executive Summary, Where Sun Meets Water. Washington, DC. https://doi.org/10.1596/31880

World Bank Group, SERIS, ESMAP, 2019. Where Sun Meets Water: Floating Solar Handbook for Practitioners, Where Sun Meets Water. Washington, DC. https://doi.org/10.1596/32804

Ziar, H., Prudon, B., Lin, F.V., Roeffen, B., Heijkoop, D., Stark, T., Teurlincx, S., Senerpont Domis, L., Goma, E.G., Extebarria, J.G., Alavez, I.N., Tilborg, D., Laar, H., Santbergen, R., Isabella, O., 2021. Innovative floating bifacial photovoltaic solutions for inland water areas. Prog. Photovoltaics Res. Appl. 29, 725–743. https://doi.org/10.1002/pip.3367

Supplemental Information

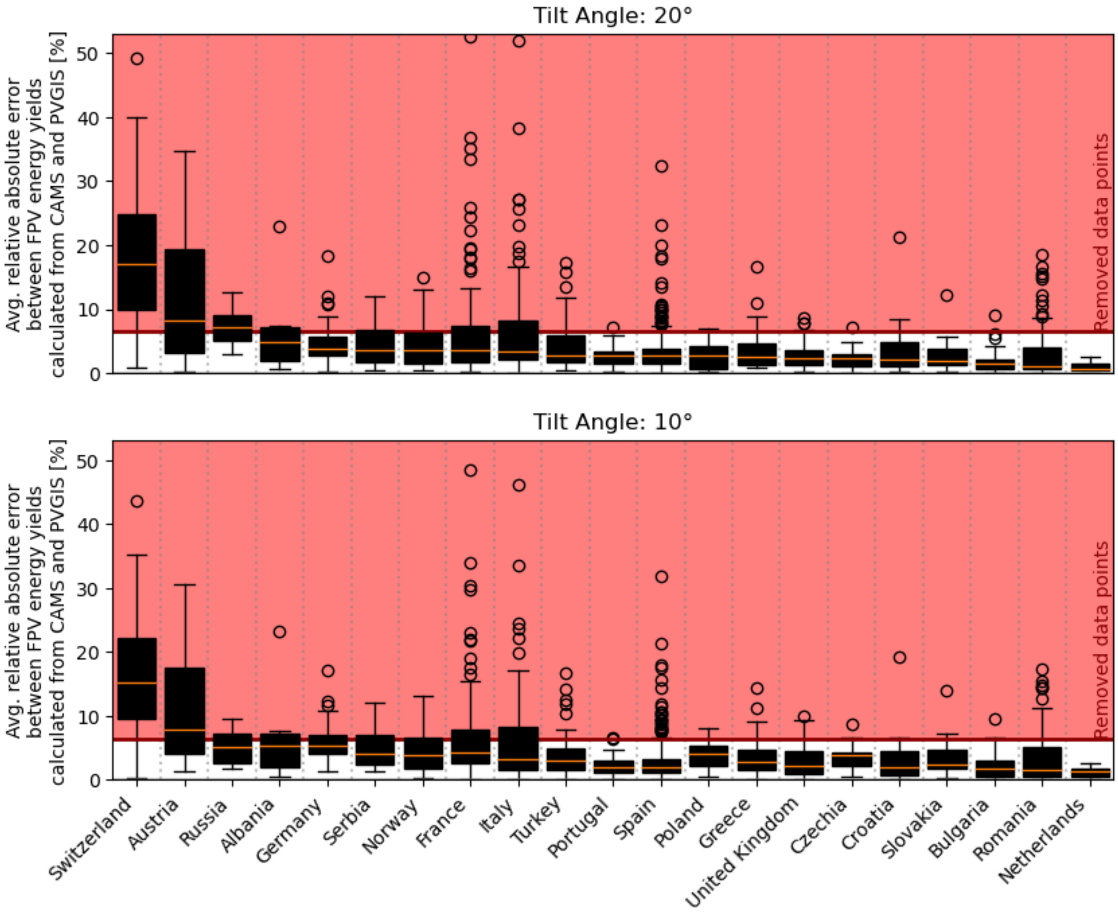

Fig. S 1. Relative difference between the FPV energy yields calculated with CAMS and PVGIS_SARAH data. Each data point is calculated as average of the energy yields calculated with two U-values. All sites where the difference was greater than 6.5% in at least one scenario were removed (i.e., those located in the red portion of the plots).

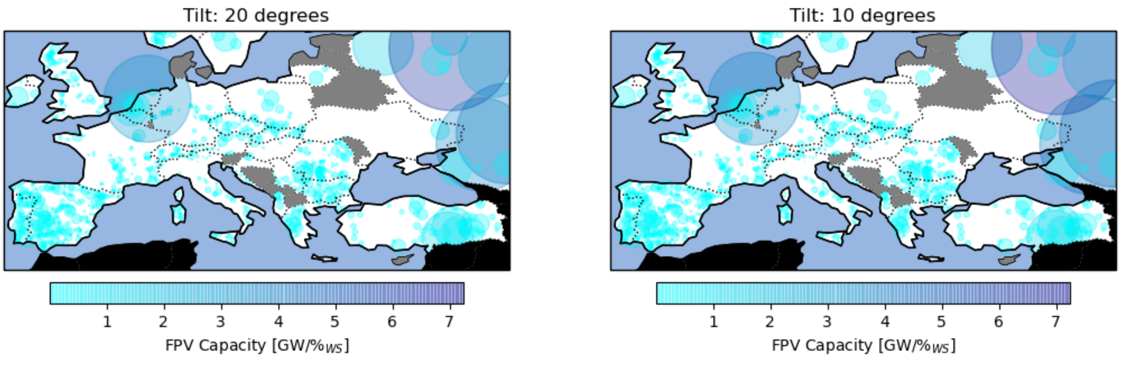

Fig. S 2. Distribution of potential FPV capacity, assuming coverage of 1% of the water surface. Only sites left after filtering are shown. In black: countries not included in the analysis. In grey: countries with no water surface available after filtering. Left plot: tilt angle of 20°. Right plot: Tilt angle of 10°. The markers are colored and sized according to the estimated capacity.

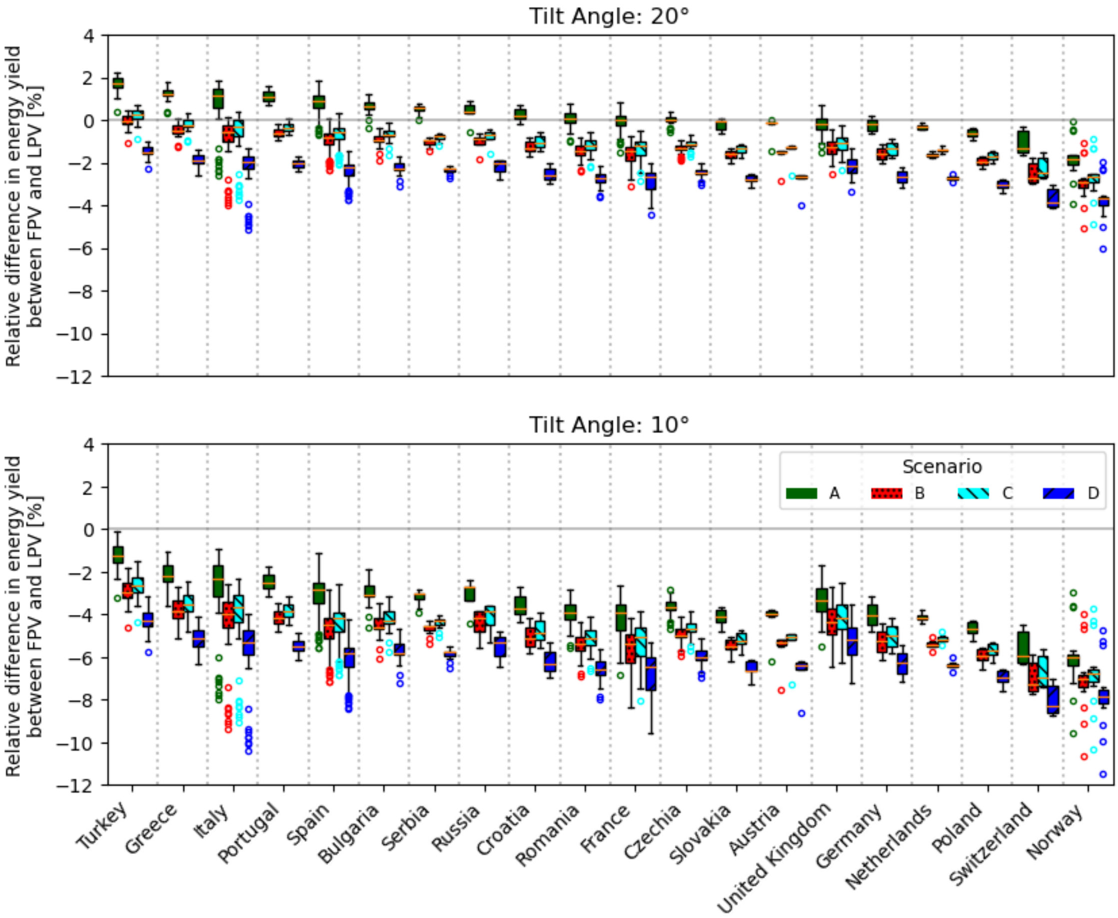

Fig. S 3. Distribution of relative energy yield gain per country depending on the scenario. The boxplot does not include countries with less than 5 data points. Positive values mean that FPV over-perform optimally tilted LPV. The countries are ordered according to the median value of Scenario A at 20° tilt.

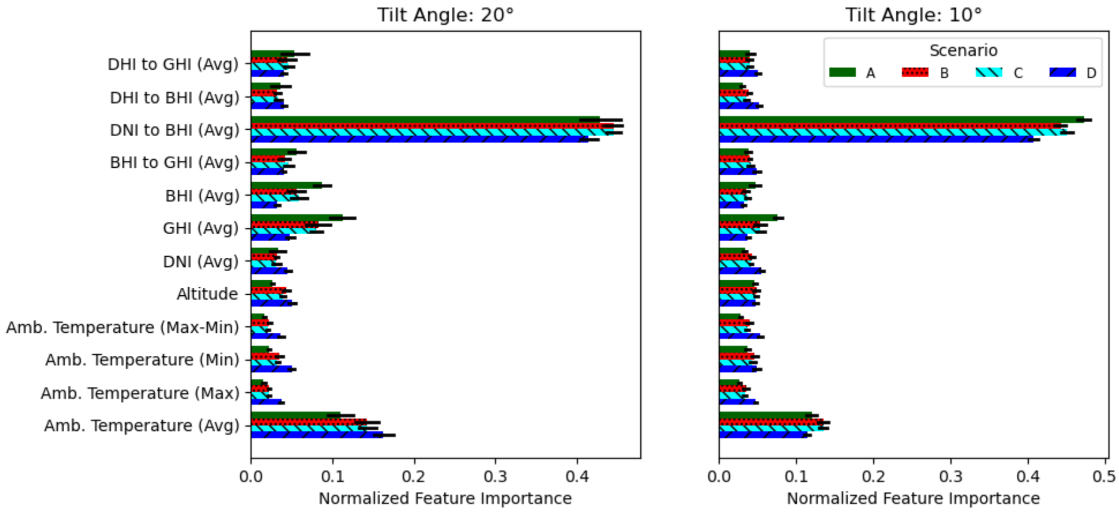

Fig. S 4. Results of a feature importance analysis. The feature importance assigns to each variable a value, whose cumulative sum is 1: the greater its value, the more impactful the variable. The analysis is conducted using an extra-trees regressor available in Python's Scikit-learn tool (Pedregosa et al., 2011)*: the bars show the mean value and the standard deviation obtained after 10 iterations.*

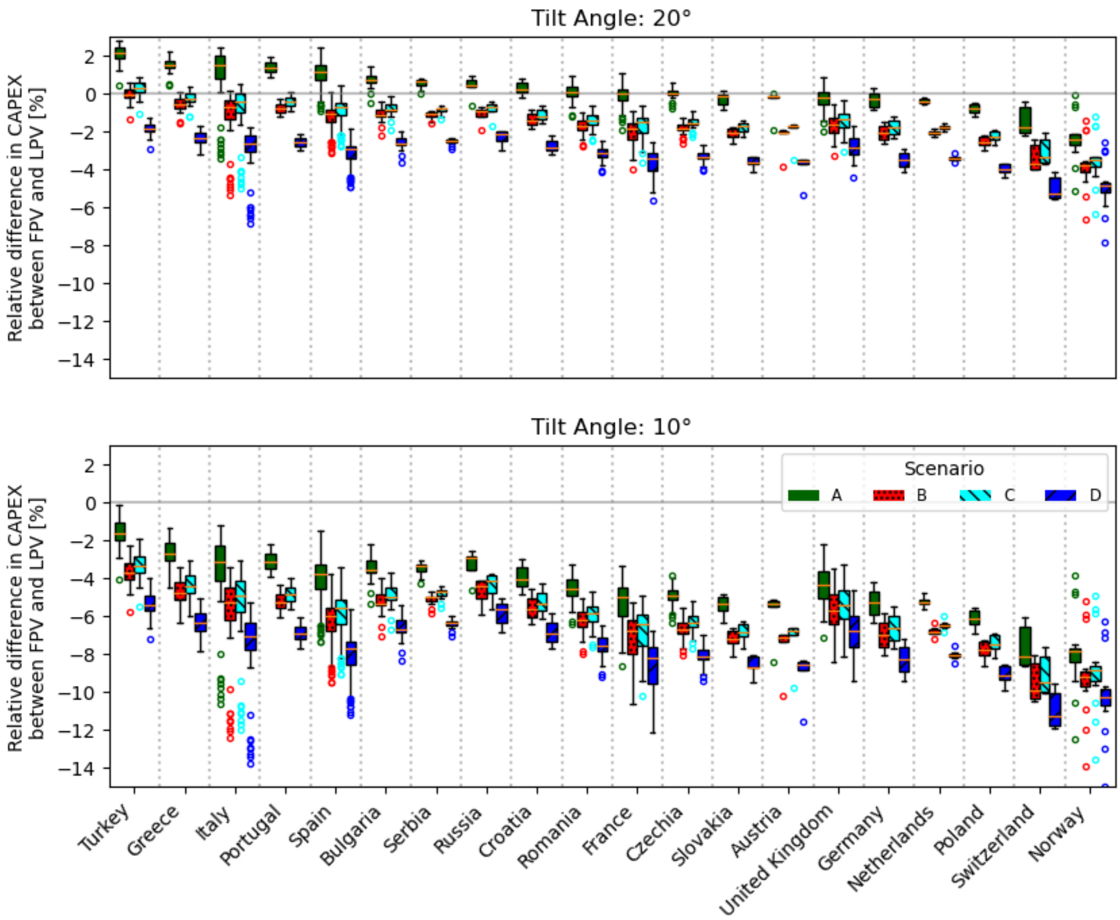

Fig. S 5. Distribution by country of the relative difference in FPV CAPEX compared to LPV. The boxplot does not include countries with less than 5 data points. Positive values mean that FPV is allowed higher CAPEX than optimally tilted LPV. Countries are ordered as in Fig. S 3.

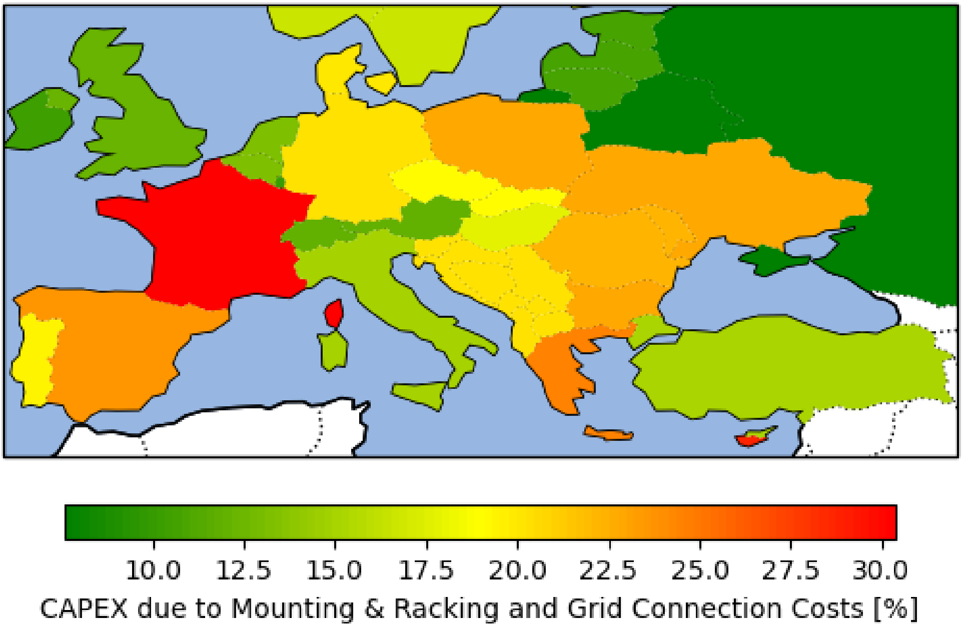

Fig. S 6. Weight of racking & mounting and grid connection costs on PV capital expenditure in 2020. Calculated from the data available in the IRENA Renewable Cost Database (IRENA, 2021)*.*

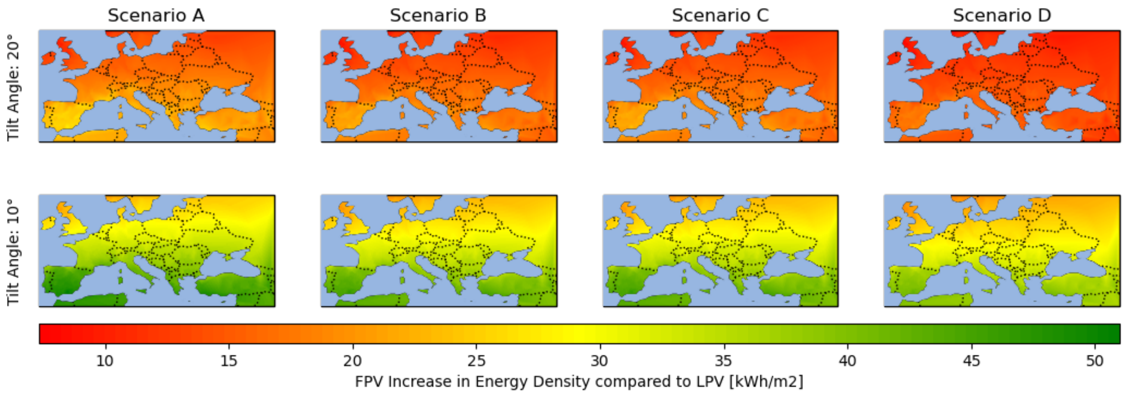

Fig. S 7. Variation in energy density between FPV and LPV, due to the FPV low tilt angles. The calculation takes into account the lower spacing needed to avoid mutual shadings at low tilts.

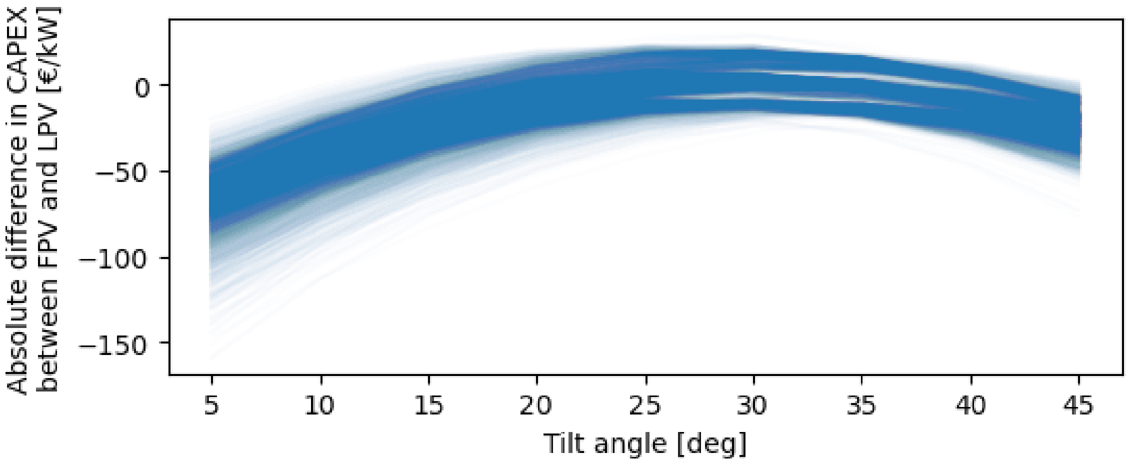

Fig. S 8. Variation in CAPEX difference between FPV and LPV depending on the tilt angle. Positive values mean that FPV is allowed higher CAPEX than optimally tilted LPV. Trends of all the data points are shown.

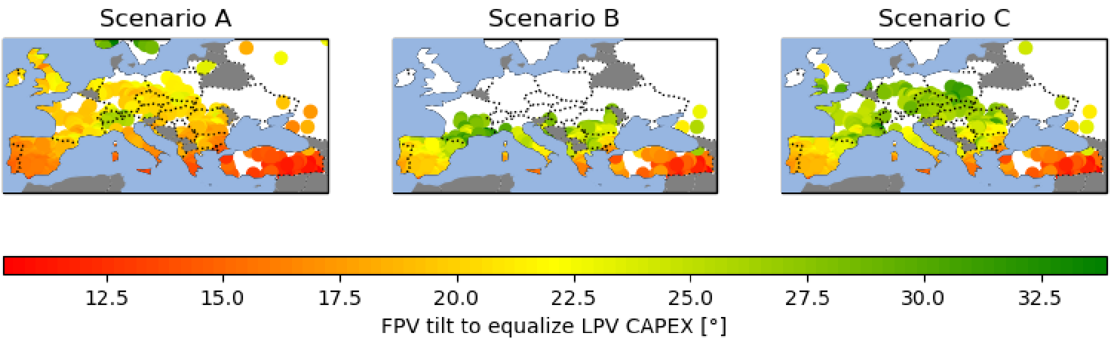

Fig. S 9. Tilt at which FPV equalizes the CAPEX of LPV. Data are not shown (i.e., white) if the FPV CAPEX are always lower than the LPV CAPEX.

Table S 1. Economic parameters used and generated for this study. Where not available, d_s has been set equal to the European mean value (6.9%). Other missing parameters were set equal to the values of nearby countries. Values originally reported in USD have been converted into EUR assuming the 2020 average conversion factor of 1.1422 $/€ (European Central Bank, n.d.)*. The CAPEX of United Kingdom was extracted from* (International Renewable Energy Agency, 2019)*.*

Country	Avg. nominal lending interest rate in 2010-20 [i_l, %] (The World Bank, n.d.; Trading Economics, 2018)	Avg. Inflation in 2010-2020 [i, %] (The World Bank, n.d.)	Nominal equity IRR in 1900-2010 [d_s, %] (Dimson et al., 2011)	Corporate Tax Rate [Tx, %] (KPMG, n.d.; Trading Economics, n.d.)	WACC [%]	CAPEX [€/kW] (IRENA, 2021)	OMEX [€/kW] (IRENA , 2021)
Albania	8.5	1.4	15.8	15.0	10.4	907.1	8.1
Austria	4.5	1.8	8.7	25.0	5.6	632.5	15.4
Belgium	4.1	1.7	6.9	25.0	4.7	935.6	15.4
Bulgaria	7.4	1.6	8.5	10.0	7.4	646.5	8.1
Croatia	9.5	1.1	8.0	18.0	7.9	907.1	8.1
Czechia	4.5	1.8	8.7	19.0	5.8	624.8	15.4
Finland	3.9	1.2	10.5	20.0	6.2	754.0	15.4
France	4.8	1.1	6.8	26.5	4.8	824.9	15.4
Germany	4.7	1.3	9.4	30.0	5.8	612.4	15.4
Greece	7.0	0.5	10.5	24.0	7.4	664.6	15.4
Hungary	4.3	2.6	9.5	9.0	6.2	825.8	15.4
Ireland	5.0	0.5	7.0	12.5	5.5	1076.7	15.4
Italy	4.0	1.1	7.2	24.0	4.8	683.4	15.4
Lithuania	6.0	1.8	8.7	15.0	6.3	1050.0	15.4
Netherlands	1.7	1.6	8.7	25.0	4.6	935.6	15.4
Norway	3.4	2.0	9.2	22.0	5.4	754.0	15.4
Poland	6.1	1.8	8.7	19.0	6.5	666.1	15.4
Portugal	5.0	1.1	8.0	21.0	5.6	818.7	15.4
Romania	8.6	2.8	9.7	16.0	8.2	674.7	8.1
Russia	10.2	6.5	20.2	20.0	12.5	1653.7	8.1
Serbia	8.3	4.1	19.7	15.0	11.7	907.1	8.1
Slovakia	5.2	1.6	10.4	21.0	6.7	624.8	15.4
Spain	4.9	1.1	6.9	25.0	5.1	666.2	15.4
Sweden	3.7	1.1	9.8	20.6	5.8	754.0	15.4
Switzerland	2.7	0.0	6.1	14.9	4.0	632.5	15.4
Turkey	19.0	10.1	17.0	25.0	15.2	723.8	15.4
Ukraine	17.7	11.7	18.6	18.0	15.9	666.1	8.1
United Kingdom	0.5	2.0	9.2	19.0	4.4	890.8	15.4